JOURNAL OF VIROLOGY, June 2007, p. 5527–5536 Vol. 81, No. 11
0022-538X/07/$08.00+0 doi:10.1128/JVI.02586-06

Generation and Characterization of a Recombinant Vesicular Stomatitis Virus Expressing the Glycoprotein of Borna Disease Virus▽

Mar Perez,[1] Roberto Clemente,[1] Clinton S. Robison,[2]† E. Jeetendra,[2]‡ Himangi R. Jayakar,[2] Michael A. Whitt,[2] and Juan C. de la Torre[1]*

Department of Molecular Integrative Neuroscience, The Scripps Research Institute, La Jolla, California 92037,[1] and Department of Molecular Sciences, University of Tennessee Health Science Center, Memphis, Tennessee 38163[2]

Received 22 November 2006/Accepted 7 March 2007

Borna disease virus (BDV) is an enveloped virus with a nonsegmented negative-strand RNA genome whose organization is characteristic of mononegavirales. However, based on its unique genetics and biological features, BDV is considered to be the prototypic member of a new virus family, *Bornaviridae*, within the order *Mononegavirales*. BDV cell entry occurs via receptor-mediated endocytosis, a process initiated by the recognition of an as yet unidentified receptor at the cell surface by the BDV surface glycoprotein (G). The paucity of cell-free virus associated with BDV infection has hindered studies aimed at the elucidation of cellular receptors and detailed mechanisms involved in BDV cell entry. To overcome this problem, we generated and characterized a replication-competent recombinant vesicular stomatitis virus expressing BDV G (rVSVΔG*/BDVG). Cells infected with rVSVΔG*/BDVG produced high titers (10^7 PFU/ml) of cell-free virus progeny, but this virus exhibited a highly attenuated phenotype both in cell culture and in vivo. Attenuation of rVSVΔG*/BDVG was associated with a delayed kinetics of viral RNA replication and altered genome/N mRNA ratios compared to results for rVSVΔG*/VSVG. Likewise, incorporation of BDV G into virions appeared to be restricted despite its high levels of expression and efficient processing in rVSVΔG*/BDVG-infected cells. Notably, rVSVΔG*/BDVG recreated the cell tropism and entry pathway of bona fide BDV. Our results indicate that rVSVΔG*/BDVG represents a unique tool for the investigation of BDV G-mediated cell entry, as well as the roles of BDV G in host immune responses and pathogenesis associated with BDV infection.

Borna disease virus (BDV) causes central nervous system (CNS) disease in a variety of vertebrate species, frequently manifested by behavioral abnormalities (31). BDV was originally identified as the causative agent of Borna disease, an often fatal immune-mediated neurological disease naturally occurring mainly in horses and sheep within regions of endemicity in central Europe (31). Current epidemiological data, however, indicate that the natural host range, prevalence, and geographic distribution of BDV are broader than originally thought (8, 16, 20, 29). Experimentally, BDV has a wide host range, from birds to rodents and nonhuman primates (8, 10, 16, 20, 29). Both host and viral factors contribute to a variable period of incubation and significant heterogeneity in the symptoms and pathology associated with infection (8, 10, 16, 20, 29).

BDV is an enveloped virus with a nonsegmented negative-strand RNA genome with a characteristic mononegavirales organization (4, 34, 35). However, based on its unique genetics and biological features, BDV is considered to be the prototypic member of a new virus family, *Bornaviridae*, within the order *Mononegavirales*. The BDV genome (ca 8.9 kb) contains six major open reading frames (ORFs) in the order 3′-N-p10/P-M-G-L-5′ (4, 34, 35). These ORFs code for the virus nucleoprotein (N), phosphoprotein (P) transcriptional activator, matrix (M), surface glycoprotein (G), and RNA-dependent RNA polymerase (L) found in other mononegavirales. The p10 open reading frame (ORF) encodes a nonstructural polypeptide of 10 kDa (p10) that is present in BDV-infected cells (40).

BDV is noncytolytic and highly neurotropic (10, 15, 16). Although viral RNA and proteins are readily detectable in BDV-infected cells, production of cell-free virus is conspicuously absent and cell-associated infectivity is extremely low (0.05 to 0.1 focus-forming unit [FFU]/cell). Notably, BDV propagates rapidly within the CNS and cultured cells in the absence of detectable assembled virions. These findings led to the view that BDV dissemination involves an initial cell penetration mediated by specific cellular receptors, followed by cell-to-cell spread.

BDV provides an important model for the investigation of viral persistence in the CNS and associated disorders (19, 25–27, 32). Studies on BDV are contributing to the elucidation of immune-mediated pathological events involved in virally induced neurological disease, as well as the mechanisms whereby viruses induce neurodevelopmental and behavioral disturbances in the absence of the hallmarks of cytolysis and inflammation. The elucidation of the mechanisms underlying the bases of BDV persistence and its effects on brain cell functions will ultimately require a detailed understanding of the mechanisms governing BDV cell tropism within the CNS, as well as signaling pathways triggered at the cell surface through binding of the virus to the receptor.

BDV G has been implicated both in cell entry by receptor-

* Corresponding author. Mailing address: The Scripps Research Institute, IMM6, 10550 N. Torrey Pines Rd., La Jolla, CA 92037. Phone: (858) 784-9462. Fax: (858) 784-9981. E-mail: juanct@scripps.edu.

† Current address: Dept. of Biological Sciences & Pittsburgh NMR Center for Biomedical Research, Carnegie Mellon University, Mellon Institute, 4400 Fifth Ave., Pittsburgh, PA 15213.

‡ Current address: GTx, Inc., 3 N. Dunlap St., Memphis, TN 38163.

▽ Published ahead of print on 21 March 2007.

mediated endocytosis (13, 14) and in cell-to-cell propagation (1). The BDV G gene directs the synthesis of a polypeptide with a predicted molecular mass of 56 kDa, but due to its extensive glycosylation it migrates with an M_r of 84,000 to 94,000 (GPC). GPC is posttranslationally cleaved by the cellular subtilisin-like protease furin (14, 28). The C-terminus product (GP2) is readily detected in virally infected cells and migrates with an M_r of 43,000. In contrast, detection of the predicted N-terminal product (GP1) of G has been difficult due to its high content of N glycans, which shield antigenic sites recognized by antibodies (18). GPC accumulates in the endoplasmic reticulum and perinuclear region, but it is typically not detected on the plasma membrane, whereas GP2 accumulates at the cell surface (13). Intriguingly, both GPC and GP2 are associated with infectious BDV particles (13).

Studies aimed at identifying BDV candidate cellular receptors have been jeopardized by the inability to grow cell-free infectious BDV to high titers. We have described the use of a pseudotype approach based on the prototypic rhabdovirus vesicular stomatitis virus (VSV) to examine the role of BDV G in virus cell entry (23). Pseudotyped viruses are competent for one single round of infection, and therefore new stocks need to be produced by *trans* complementation, via transfection, with the glycoprotein of interest. Replication-competent recombinant VSV (rVSV) expressing heterologous glycoproteins has been documented (17, 21) and has proved to be a far more powerful tool for investigating the role of viral glycoproteins in infection in both cell culture and whole organisms. Here we describe the generation and characterization of an rVSV (rVSVΔG*/BDVG) in which the VSV G gene was replaced by the coding region for green fluorescent protein (GFP) and the BDV G gene was incorporated as an additional ORF between the M and GFP ORFs of rVSVΔG*/BDVG. We present evidence that rVSVΔG*/BDVG recreates the tropism and mechanism of cell entry exhibited by the bona fide BDV. We also show that rVSVΔG*/BDVG is highly attenuated both in cell culture and in vivo. We discuss the implications of these findings for the identification of cellular receptors of BDV and the investigation of the effects of BDV G on the biology of virally infected cells.

MATERIALS AND METHODS

Cells. Baby hamster kidney BHK-21 cells (ATCC CCL 10) were maintained in high-glucose Dulbecco's modified Eagle medium (DMEM) supplemented with 10% heat-inactivated fetal calf serum (FCS) (Life Technologies), 2 mM glutamine, and 0.1× tryptose phosphate broth (Life Technologies). Vero cells were maintained in minimal essential medium supplemented with 2 mM glutamine and 7% heat-inactivated FCS. MC57 cells, a mouse fibroblast cell line, were maintained in RPMI 1640 medium supplemented with 2 mM glutamine and 7% heat-inactivated FCS.

Generation of recombinant virus. To generate rVSVΔG*/BDVG, the BDV G ORF was amplified from pC-p56 (23) with primers OG1FMluI (5′-CGCACGC GTGCCATGGAGCTTTCAATGTCTTCTCTTATCG-3′) and OG1509RNheI (5′-CCTAGCTAGCTTATTCCTGCCACCGGCCGAGG-3′) and the PCR fragment cloned into the MluI and NheI sites of the VSVΔG-PL/GFP2.6 vector, where the VSV G ORF had been replaced by the GFP ORF (38). The recombinant virus was recovered following established protocols (30, 37, 38). Briefly, BHK-21 cells were infected with vTFT7.3, a recombinant vaccinia virus expressing the phage T7 RNA polymerase (9). After 1 h, plasmids encoding VSV N, P, G, and L proteins were cotransfected together with the full-length cDNA clone of the VSV genome (Indiana serotype) containing BDV G as an additional VSV ORF. The supernatant fluid was harvested 48 h after transfection, filtered to remove vTFT7.3, and used to infect BHK-21 cells *trans* complemented with VSV G to enhance the efficiency of virus rescue. Cells were examined for GFP expression 24 h after infection to assess virus rescue. The virus recovered from this second infection was plaque purified three times in BHK-21 cells expressing VSV G and then passed three times on Vero cells to assure that the viral preparation was clean of VSV G. The G gene in rVSVΔG*/BDVG was sequenced and found to be identical to the parental BVD G gene. The virus was propagated on Vero cells. A Vero cell plaque assay was used to quantify infectivity. The generation of rVSVΔG*/LCMVG has been described previously (24).

Antibodies. Anti-BDV antibodies used included rabbit polyclonal antibodies against BDV nucleoprotein (Ab-N) and glycoprotein (Ab-G and Ab-$GP1_N$). Ab-N was generated by immunization with bacterially expressed N. Ab-G was generated by immunization against a bacterially expressed truncated form of the BDV p56 glycoprotein (14). Ab-$GP1_N$ was generated as described elsewhere (2a). To detect the nucleocapsid protein of VSV, we used a murine monoclonal antibody (10G4; Ab-VSV N). Lymphocytic choriomeningitis virus (LCMV) was neutralized using a monoclonal anti-GP2 antibody, 83.6 (39).

IF microscopy. Infected-cell monolayers were washed with phosphate-buffered saline, fixed with methanol:acetone (1:1) for 5 min, and processed for immunofluorescence (IF) as described previously (23). Briefly, after blocking with 10% normal goat serum for 45 min at room temperature, cells were stained with primary antibodies for an hour. Secondary fluorescent antibodies used were Rhodamine Red-X-labeled anti-mouse immunoglobulin G (IgG) or anti rabbit IgG. The coverslips were mounted on microscope slides with Mowiol and viewed with a fluorescence microscope.

Incorporation of BDV G polypeptides into VSV particles. Culture medium supernatant (tissue culture supernatant [TCS]) was harvested from Vero cells infected with rVSVΔG*/BDVG (multiplicity of infection [MOI] = 5 to 10). The TCS was clarified by centrifugation at low speed and viral particles collected by ultracentrifugation through a 20% sucrose cushion (prepared in 50 mM Tris [pH 7.5]–150 mM NaCl). Viral particles in the high-speed pellet were analyzed by Western blotting using Ab-G and Ab-$GP1_N$.

Western blotting. For Western blot analysis, cells were harvested in sample buffer (50 mM Tris-HCl [pH 6.8], 2% sodium dodecyl sulfate [SDS], 0.1% bromophenol blue, 10% glycerol, 100 mM dithiothreitol). Cell lysates were separated by SDS-polyacrylamide gel electrophoresis (PAGE) (10% polyacrylamide) by using the buffer system of Laemmli, and the proteins were transferred onto Immobilon-P membranes (Millipore, Bedford, MA) as described previously (33). Immunodetection of the proteins was done by using the SuperSignal West Pico chemiluminescent substrate system (Pierce, Rockford, IL).

Analysis of RNA by Northern blot hybridization and RT-PCR. RNA was isolated from cells and tissues by using TriReagent (Molecular Research Center, Cincinnati, OH) according to the manufacturer's instructions. Northern blots were prepared with appropriate ^{32}P-labeled DNA probes. Autoradiogram films were scanned with a GS-800 densitometer (Bio-Rad) and analyzed with Image Quant image analysis software (Molecular Dynamics, Palo Alto, CA). Once an image had been acquired, optimization to reduce noise or background was performed and the bands were quantified. Reverse transcription-PCR (RT-PCR) was carried out using Superscript II and random hexamer primers for the RT reaction and *Taq* polymerase together with VSV N- or actin-specific primers.

Apoptotic analysis. Vero cells were either mock infected or infected with the recombinants at a MOI of 5. At the different times postinfection, cells were washed and subsequently incubated for 15 min with Annexin V-fluorescein isothiocyanate and 7-amino-actinomycin D according to the manufacturer's instructions (Pharmingen). After staining, cells were immediately acquired with a FACSCalibur flow cytometer (Becton Dickinson) and then analyzed with FlowJo (Treestar) software.

Metabolic labeling of infected cells and virus. For metabolic labeling of the rVSV proteins, 10^6 Vero cells were infected with wild-type (wt) VSV or rVSV (MOI = 10). After 4 h, cells were washed with methionine-free DMEM and incubated for 14 h at 37°C in 0.5 ml methionine-free DMEM containing 100 mCi of [^{35}S]methionine-cysteine (Tran^{35}S-label; ICN) and 10% DMEM. Protein lysates were separated by SDS-PAGE. Labeled viral particles were collected by ultracentrifugation of the clarified culture medium supernatant through a 20% sucrose cushion (prepared in 50 mM Tris [pH = 7.5]–150 mM NaCl).

Titration of infectious virus. Virus titers were determined by plaque assay. Vero cell monolayers (80% confluent) were incubated with 10-fold serial dilutions of viral stocks for 90 min at 37°C. After removal of the inoculum, cells were washed with minimal essential medium, overlaid with agarose (Seakem ME) in medium 199 (Invitrogen) supplemented with 1% FCS, 100 units/ml penicillin, and 100 μg/ml streptomycin. Cultures were fixed with 25% paraformaldehyde in phosphate-buffered saline, and plaques were visualized by 1% crystal violet staining. For titration of rVSVΔG*/BDVG, the overlay medium contained 0.5%

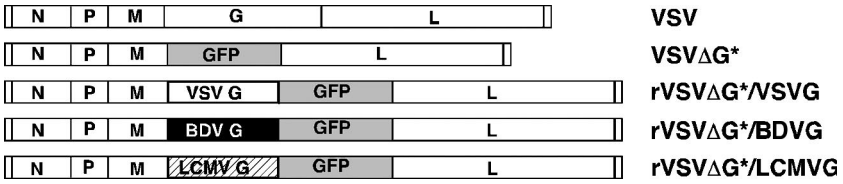

FIG. 1. Schematic representation of the wt and recombinant VSV genomes. The indicated rVSVs were generated by cloning the ORF coding for the indicated G of interest upstream of the GFP ORF in VSVΔG*.

agarose, whereas for titration of rVSVΔG*/LCMVG and rVSVΔG*/VSVG, the agarose concentration was raised to 1%.

Neutralization assay. Aliquots (1,000 PFU) of the indicated rVSV were incubated for 45 min at 37°C with the neutralizing antibodies (Nt-Ab) targeting the appropriate viral surface glycoprotein (G) and assayed for infectivity by plaque assay. Infectivity was normalized with respect to values obtained with each rVSV incubated under the same conditions but in the presence of 5% normal goat serum instead of Nt-Ab.

Infection of mice and rats. Adult male (2 to 3 months old) wt C57BL/6 (B6) mice, B6 mice lacking a functional type I interferon receptor ($IFNAR^{-/-}$ mice), and newborn rats (Lewis strain) were used for intracranial (i.c.) injections (30-μl volume). Experiments were performed under specific-pathogen-free conditions according to guidelines of the Institutional Animal Care and Use Committee at The Scripps Research Institute.

Detection of viral antigen by immunohistochemistry (IHC). Brains from mice and rats infected with the indicated rVSV and from mock-infected controls were collected, embedded in Tissue-Tek O.C.T. compound, and frozen on dry ice. Cryosections (6 μm) were cut, placed on Fisher Superfrost Plus slides, dried, and fixed with 2% formaldehyde. After a blocking step with donkey anti-mouse anti-IgG, sections were stained with a mouse monoclonal antibody to VSV N. After the primary antibody incubation, sections were washed, stained for 1 h at room temperature with a biotinylated secondary antibody (Jackson ImmunoResearch Laboratories), washed, and stained with streptavidin–Rhodamine Red-X (Jackson ImmunoResearch Laboratories). All sections were costained for 5 min at room temperature with 1 μg/ml 4′,6′-diamidino-2-phenylindole (Sigma-Aldrich) to visualize cell nuclei. Brain tissue sections from rats were also examined by IHC for expression of glial acidic fibrillary protein (GFAP) and lectin to identify astrocyte and microglia cells within the brain parenchyma.

RESULTS

Generation and growth properties of rVSVΔG*/BDVG. To generate rVSVΔG*/BDVG, we followed published protocols (37, 38), and detailed descriptions are provided in Materials and Methods (Fig. 1). The generation of rVSVΔG*/LCMVG has been described previously (24), as has that of rVSVΔG*/VSVG (38).

To examine the single-step growth properties of rVSVΔG*/BDVG, we infected Vero cells (MOI = 3), and at various times after infection we determined titers of infectious virus in TCS by plaque assay (Fig. 2A). We also infected Vero cells (MOI = 3) with rVSVΔG*/VSVG and rVSVΔG*/LCMVG (Fig. 2A). Cells infected with rVSVΔG*/BDVG exhibited a delayed kinetics and low level of total infectious virus compared to cells infected with either rVSVΔG*/VSVG or rVSVΔG*/LCMVG. Consistent with this finding, the kinetics of cell death associated with rVSVΔG*/BDVG infection was significantly delayed compared to that for cells infected with rVSVΔG*/VSVG or rVSVΔG*/LCMVG (Fig. 2B). Likewise, plaques produced by rVSVΔG*/BDVG were smaller in size and took longer to develop than those produced by rVSVΔG*/VSVG (Fig. 2C).

Synthesis of viral RNA in rVSVΔG*/BDVG-infected cells. The differences in the single-step growth properties observed between rVSVΔG*/VSVG and rVSVΔG*/BDVG led us to examine whether these viruses also exhibited differences in virus RNA replication and transcription. For this, we isolated total cell RNA from the same samples used to determine production of infectious virus (Fig. 2A), and equal amounts of RNA of each sample were analyzed by Northern blot hybridization using a double-stranded-DNA probe specific to VSV N (Fig. 3). Cells infected with rVSVΔG*/BDVG exhibited a delayed kinetics in virus RNA replication compared to those infected with rVSVΔG*/VSVG and, to a lesser extent, rVSVΔG*/LCMVG (Fig. 3). Moreover, genome/N-mRNA ratios were significantly lower in rVSVΔG*/BDVG-infected cells than in rVSVΔG*/VSVG- and rVSVΔG*/LCMVG-infected cells, which correlated with increased levels of N mRNA in rVSVΔG*/BDVG-infected cells (Fig. 3). RNA isolated from rVSVΔG*/VSVG-infected cells at 48 h postinfection (p.i.) produced only very weak Northern blot hybridization signals for both N mRNA and genomic RNA, which correlated with a dramatic decrease in levels of 28S rRNA (not shown), which was due to the robust cytopathic effect caused by rVSVΔG*/VSVG.

Biosynthesis and virion incorporation of viral polypeptides produced in rVSVΔG*/BDVG-infected cells. We examined the biosynthesis of BDV G polypeptide species in rVSVΔG*/BDVG-infected cells and their incorporation into rVSV particles. For this, we infected Vero cells with rVSVΔG*/BDVG (MOI = 10), and at 4 h p.i., cells were radiolabeled with Trans^{35}S-label (200 μCi/ml). After 18 h of labeling, we harvested TCS and prepared whole-cell extracts (WCE) for each sample. TCS samples were clarified by centrifugation at low speed and viral particles collected by ultracentrifugation through a sucrose (20%) cushion. We used equal amounts of radioactivity (cpm) from each WCE sample and from each virion particle sample recovered in the high-speed pellet for SDS-PAGE followed by autoradiography. WCE and concentrated virions from cells infected with each of the rVSVs exhibited the predicted similar patterns of VSV polypeptide synthesis with the exception of the glycoprotein, where each rVSV produced a polypeptide of the expected molecular size for BDV G, VSV G, and LCMV G, respectively (Fig. 4A). We next used a newly generated antiserum to the N terminus of BDV GP1 (Ab-$GP1_N$) and also a rabbit polyclonal serum to BDV G (Ab-G) (14) to examine the G species present in virions released from rVSVΔG*/BDVG-infected cells and compared them with those present in bona fide BDV virions. As a control for these studies, we used samples from rVSVΔG*/VSVG-infected cells. Consistent with our previous findings, Ab-G recognized GPC and GP2 in WCE and cell-free virions (not shown). Notably, our newly generated Ab-$GP1_N$ readily recognized GP1 in both WCE and cell-released virus prepara-

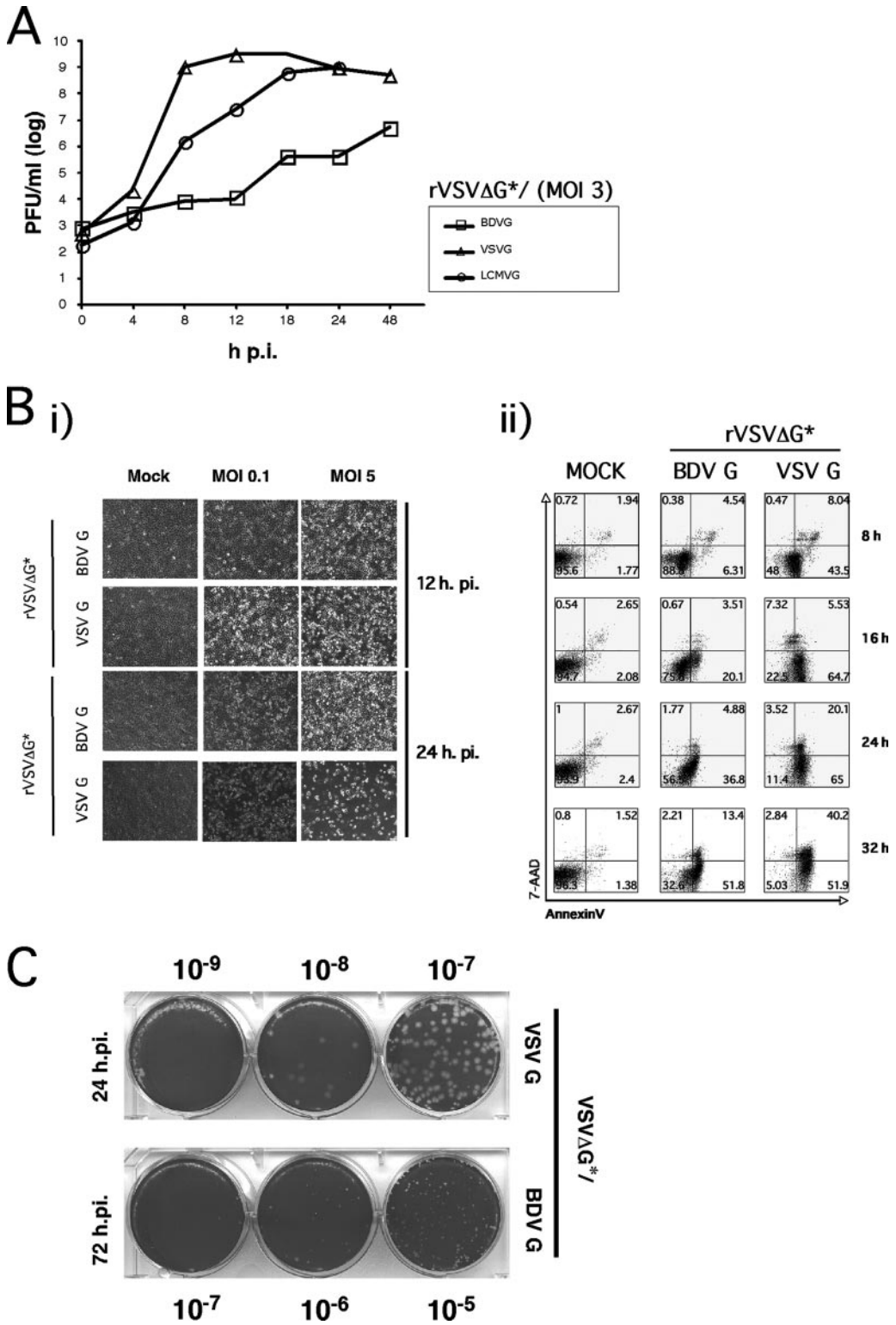

FIG. 2. Growth properties of rVSVΔG*/BDVG. (A) Single-step growth curve. Vero cells were infected at a MOI of 3 with the indicated rVSV. Virus-containing TCS were harvested at the indicated times p.i. and viral titers determined by plaque assay. (B) CPE properties of rVSV. (i) Light microscopy assessment of CPE. Vero cell monolayers were infected with the indicated rVSV at 0.1 or 5 MOI and photographed at the indicated times p.i. (ii) Kinetics and magnitude of virally induced cell apoptosis. Vero cells infected (MOI = 3) with the indicated rVSV were collected at the indicated times p.i. and subjected to fluorescence-activated cell sorting analysis using Annexin V-fluorescein isothiocyanate and 7-amino-actinomycin D. (C) Plaque development. Indicated dilutions of rVSVΔG*/VSVG or rVSVΔG*/BDVG were used to infect Vero cells. After the adsorption time (90 min at 37°C), the virus inoculum was removed and cells overlaid with agarose (1%). At 24 h or 72 h p.i., cells infected with rVSVΔG*/VSVG or rVSVΔG*/BDVG, respectively, were fixed and stained with crystal violet.

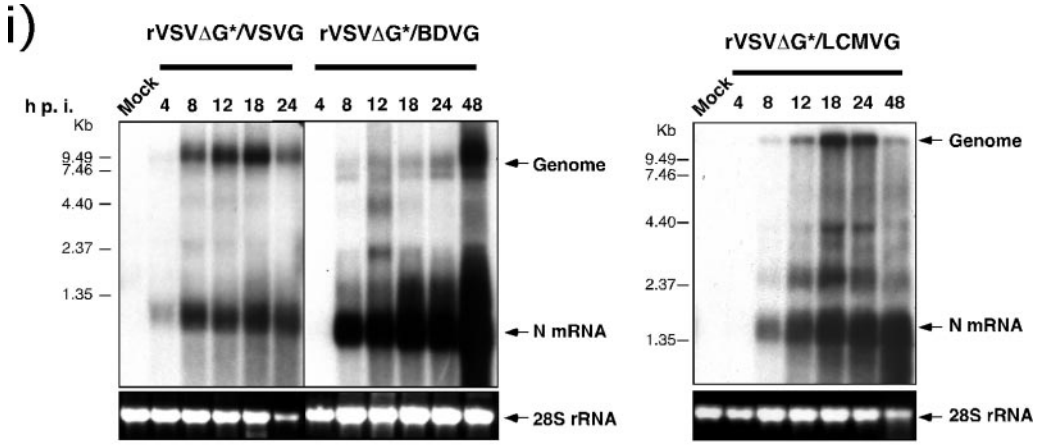

ii)

rVSVΔG*/	h.pi				
	0	4	8	12	24
BDV G	n.d.	n.d.	0.06	0.02	0.24
LCMV G	n.d.	0.05	0.57	0.71	0.63
VSV G	n.d.	n.d.	0.31	0.43	0.44

Ratio (genome RNA/messenger RNA)

FIG. 3. Altered pattern of RNA replication and gene transcription in rVSVΔG*/BDVG-infected cells. Vero cells infected with the indicated rVSV were collected at the indicated hour p.i., and their RNA was isolated and subjected to Northern blot analysis using a DNA probe for VSV N. Ethidium bromide staining of the 28S rRNA was used to assess RNA loading. Bands corresponding the VSV genome RNA and N mRNA species are indicated. Levels of N mRNA and genome RNA species were quantified by densitometry of their hybridization as described in Materials and Methods and values used to determine genome RNA/N-mRNA ratios at different times p.i.

tions from Vero cells infected with either rVSVΔG*/BDVG or BDV (Fig. 4B).

To determine if the reduced infectivity observed in the one-step growth curve (Fig. 2A) was due to reduced particle production, we compared the amount of virus released from cells infected with either rVSVΔG*/VSVG, rVSVΔG*/BDVG, or VSV G-complemented rVSVΔG* (Fig. 4C). The genome rVSVΔG* does not express an envelope glycoprotein and produces noninfectious "bald" particles corresponding to approximately 5% to 10% of the amount of virus released from wild-type VSV-infected cells. We used the same volume of TCS from cells infected with each of the viruses, concentrated virions by ultracentrifugation, and then analyzed the pelleted virus by SDS-PAGE and Coomassie staining. Particle production in rVSVΔG*/BDVG-infected cells was significantly reduced compared to that in rVSVΔG*/VSVG-infected cells but was higher than the amount of bald virus released from rVSVΔG*-infected cells. Both rVSVΔG*/VSVG and rVSVΔG*/BDVG particles exhibited the characteristic bullet shape of rhabdoviruses (not shown).

Cell tropism of rVSVΔG*/BDVG. To assess whether rVSVΔG*/BDVG recreated the cell tropism of bona fide BDV, we compared the susceptibilities to rVSVΔG*/BDVG of cell lines known to be either susceptible or resistant to BDV infection. Both BDV and rVSVΔG*/BDVG displayed the same cell tropism pattern as determined by their ability to cause cytopathic effect (CPE) in the cell lines tested (Fig. 5A). The rVSVΔG*/BDVG-induced CPE correlated with its ability to replicate within the cells as determined by detection of viral antigen expression by IF in Vero cells but not in MC57 cells (Fig.5Aii). MC57 cells were fully susceptible to infection with rVSVΔG*/VSVG, indicating that the resistance of MC57 to rVSVΔG*/BDVG was not due to an intracellular blockade of VSV multiplication. Consistent with their susceptibility to LCMV infection, both MC57 and Vero cells were susceptible to infection with VSVΔG*/LCMVG, which further supported a correlation between the virus entry phenotype and the glycoprotein present in the rVSV envelope. Results from neutralization assays provided additional evidence that envelope glycoprotein played a central role in determining cell entry of the different rVSVs (Fig. 5B).

We next asked whether rVSVΔG*/BDVG and BDV entered Vero cells using the same receptor molecule. For this, we conducted competition experiments. We added increasing amounts of UV-inactivated rVSVΔG*/BDVG or VSVΔG*/LCMVG to Vero cells. After 45 min of adsorption at 4°C (to prevent internalization), virus was removed and cells were adsorbed with wt BDV (500 FFU) for 60 min at 4°C. After several washes, cells were transferred to 37°C to induce virus internalization. Three hours later, cells were trypsinized and mixed with fresh uninfected Vero cells and 48 h later analyzed by IF using anti-BDV antibodies. BDV infectivity is cell associated, and thereby it can be assumed that 1 FFU is derived from a single initially infected cell. Incubation of cells with rVSVΔG*/BDVG but not rVSVΔG*/LCMVG resulted in a

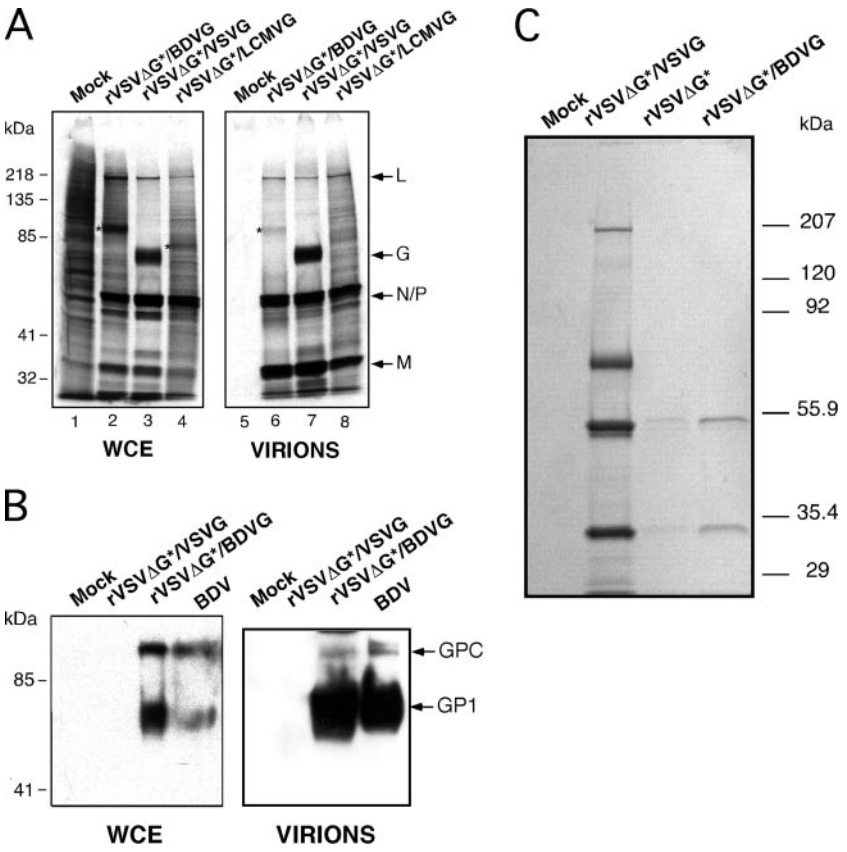

FIG. 4. Synthesis of rVSVΔG*/BDVG polypeptides in infected cells and their incorporation into virions. (A) Vero cells were infected with the indicated rVSVs and at 4 h p.i. were metabolically labeled with [^{35}S]methionine-cysteine for 18 h prior to preparation of cell lysates and protein analysis by SDS-PAGE and autoradiography. TCS from the same samples were collected, and virions were purified by ultracentrifugation through a 20% sucrose cushion. Samples were normalized by loading the same amount of radioactivity (cpm) in both cases. (B) Detection of BDV G by Western blotting. WCE and virion samples prepared from TCS of rVSV-infected cells were subjected to Western blotting using Ab-GP1$_N$. (C) Levels of particle production by cells infected with rVSV. Virions were concentrated from equivalent TCS volumes from each sample of infected cells and analyzed by SDS-PAGE followed by Coomassie staining.

dose-dependent decrease in infectivity of authentic BDV (Fig. 5C).

Virulence of rVSVΔG*/BDVG in vivo. Our results using cell culture systems indicated that rVSVΔG*/BDVG was significantly attenuated compared to rVSVΔG*/VSVG. We therefore decided to explore whether this attenuated phenotype could be extended to an in vivo infection. For this we inoculated (i.c.) B6 mice with either rVSVΔG*/BDVG or rVSVΔG*/VSVG using in each case two virus doses (100 and 1,000 PFU) (Fig. 6A). Consistent with previous reports, i.c. inoculation with rVSVΔG*/VSVG result in 100% (n = 8) mortality between days 3 and 5. In contrast, we observed 100% (n = 8) survival of mice inoculated with rVSVΔG*/BDVG (at both 100- and 1,000-PFU doses). In addition, rVSVΔG*/BDVG-infected mice did not exhibit any noticeable clinical symptoms during the entire course (15 days) of this experiment. RT-PCR studies showed that viral RNA was detected in brain tissue of rVSVΔG*/VSVG-infected mice at both days 2 and 3 p.i. (Fig. 6B). Subsequent times were not examined because all the mice had succumbed to infection by day 4 p.i. Likewise, viral RNA was readily detected in brain tissue of rVSVΔG*/BDVG-infected mice at day 2 p.i. but not at any of the later times examined (Fig. 6B). Based on these results, we examined whether, as with wt VSV, replication of rVSVΔG*/BDVG became unchecked in the absence of type I interferon responses. To this end, we inoculated (i.c.) B6 mice lacking a functional type I interferon receptor (IFNAR$^{-/-}$) with either rVSVΔG*/BDVG (1,000 PFU) or rVSVΔG*/VSVG (1,000 PFU) (Fig. 6C). Inoculation with rVSVΔG*/VSVG caused 100% mortality within 2 to 3 days, whereas mice inoculated with rVSVΔG*/BDVG remained healthy during the entire observation period, which extended up to 4 weeks for some of the mice. Unlike the situation with wt mice, we detected viral RNA sequences in brain tissue but not liver tissue of rVSVΔG*/BDVG-infected mice up to 4 weeks p.i., the latest time examined (Fig. 6D). Consistent with the detection of rVSVΔG*/BDVG RNA in brain tissue, IHC studies revealed the presence of virus antigen-positive cells (Fig. 6E). These findings indicated that rVSVΔG*/BDVG was able to persist in the CNS of IFNAR$^{-/-}$ mice.

Similarly to BDV, rVSVΔG*/BDVG also was able to replicate in brains of newborn infected rats. IHC studies showed high loads of viral antigen in both the cortex and the hippocampus of newborn rats at day 5 p.i. with rVSVΔG*/BDVG (Fig. 7A). rVSVΔG*/BDVG also exhibited attenuated virulence in rats compared to rVSVΔG*/VSVG (Fig. 7B).

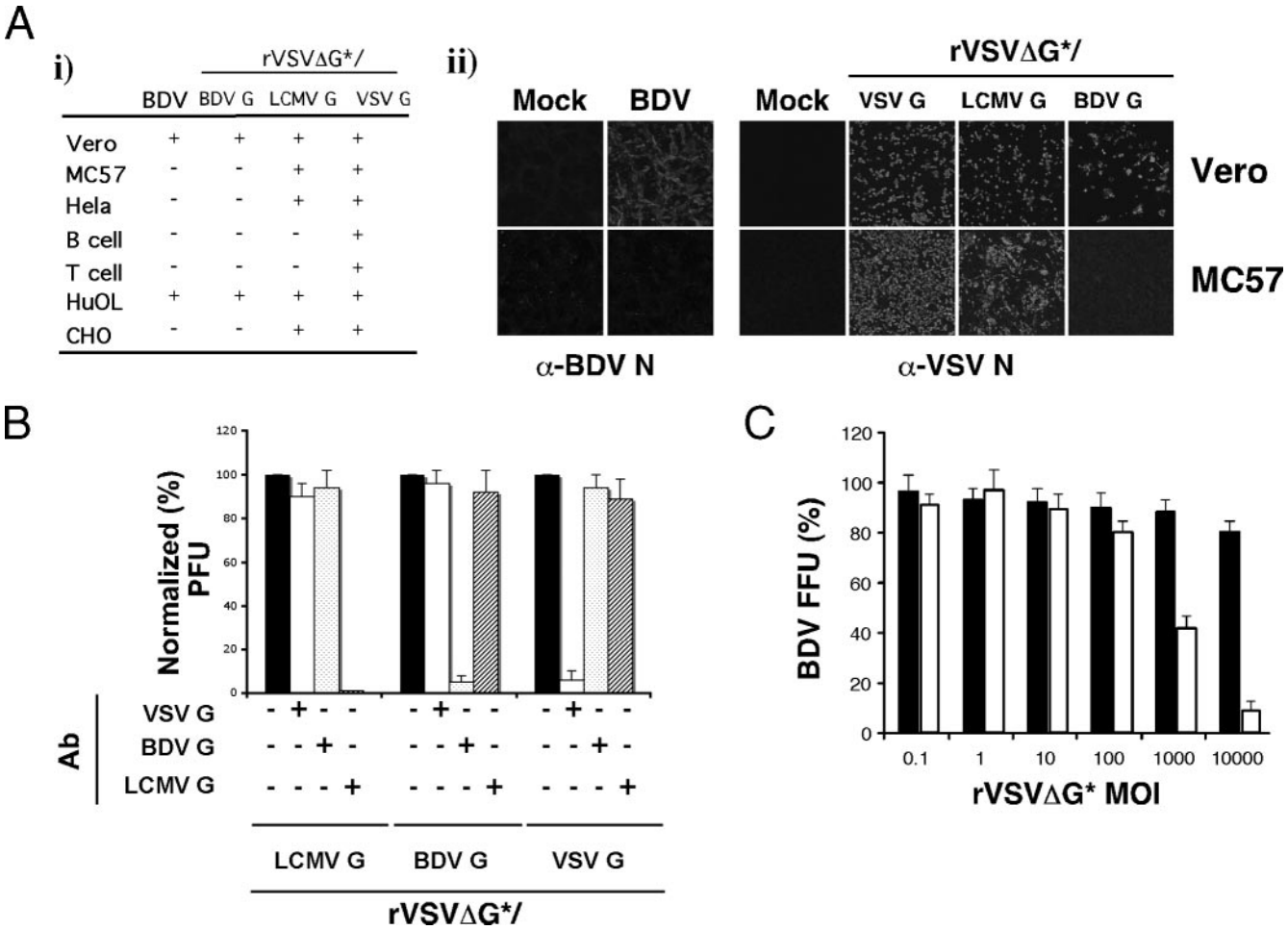

FIG. 5. rVSVΔG*/BDVG recreated the cell tropism and entry of bona fide BDV. (Ai) Susceptibility of different cell lines to CPE caused by the indicated rVSV. The indicated cell lines were infected with the indicated rVSV (MOI = 3) and CPE assessed by light microscopy at 72 h p.i. Infections that did not exhibit CPE at 72 h p.i. were allowed to proceed until day 10 p.i., a time at which the cells were considered to be nonsusceptible if they remained free of signs of CPE. (Aii) Expression of viral antigen in susceptible cells. Vero and MC57 cells were infected with the indicated rVSV (MOI = 5), and 24 h p.i., the cells were fixed and analyzed by IF with a polyclonal rabbit serum to BDV N (Ab-BDV N) or with a monoclonal antibody to VSV N (Ab-VSV N). (B) Neutralization of rVSVΔG*/BDVG by Nt-Ab to BDV G was done as described in Materials and Methods. The infectivity of the nonneutralized fraction of virus was determined by plaque assay and normalized (%) with respect to the infectivity of the corresponding rVSV treated with control serum. (C) BDV cell entry is competed by rVSVΔG*/BDVG. Increasing amounts of UV-inactivated rVSVΔG*/BDVG (open bars) or rVSVΔG*/LCMVG (solid bars) were added to Vero cells. After 45 min of adsorption at 4°C (to prevent internalization), virus was removed and cells were adsorbed with wt BDV for 60 min at 4°C. After several washes, cells were transferred to 37°C to induce virus internalization. At 3 h p.i., cells were trypsinized, mixed with fresh uninfected Vero cells, and at 48 h p.i. analyzed by IF using a polyclonal rabbit serum to BDV N. FFU values were normalized, considering 100% the FFU values obtained with samples subjected to the same protocol but being exposed to diluent instead of to treatment with UV-inactivated rVSV viruses.

DISCUSSION

The paucity of cell-free virus associated with BDV infection has hampered studies aimed at identifying receptors that facilitate BDV cell entry. The development of reverse genetics systems for BDV have provided investigators with a novel and powerful tool to investigate the molecular and cell biology, as well as pathogenesis, of BDV (5, 36). However, as with bona fide BDV isolates, the infectivity of virus rescued via reverse genetics remains extremely low and cell associated. With the aim of overcoming this problem, we took advantage of the existing robust reverse genetics for the prototypic mononegavirus VSV (22) which has allowed investigators to rescue a variety of rVSVs expressing heterologous viral glycoproteins that retain their ability to mediate receptor recognition and cell entry (12, 17, 21). In this work we have described the generation and characterization of a recombinant VSV (rVSVΔG*/BDVG) where VSV G was replaced by BDV G.

We detected high titers (ca. 10^7 PFU/ml) of infectious virus in tissue culture supernatants of rVSVΔG*/BDVG-infected cells (Fig. 2A). Although this titer was approximately 100-fold lower than that produced by the parental rVSVΔG*/VSVG, it is comparable to what has been observed with some other rVSVs expressing foreign viral glycoproteins (12). In the case of rVSVΔG*/BDVG, the lower titers probably reflect inefficient particle formation and release due to the slow release of BDV G from the endoplasmic reticulum and its limited traf-

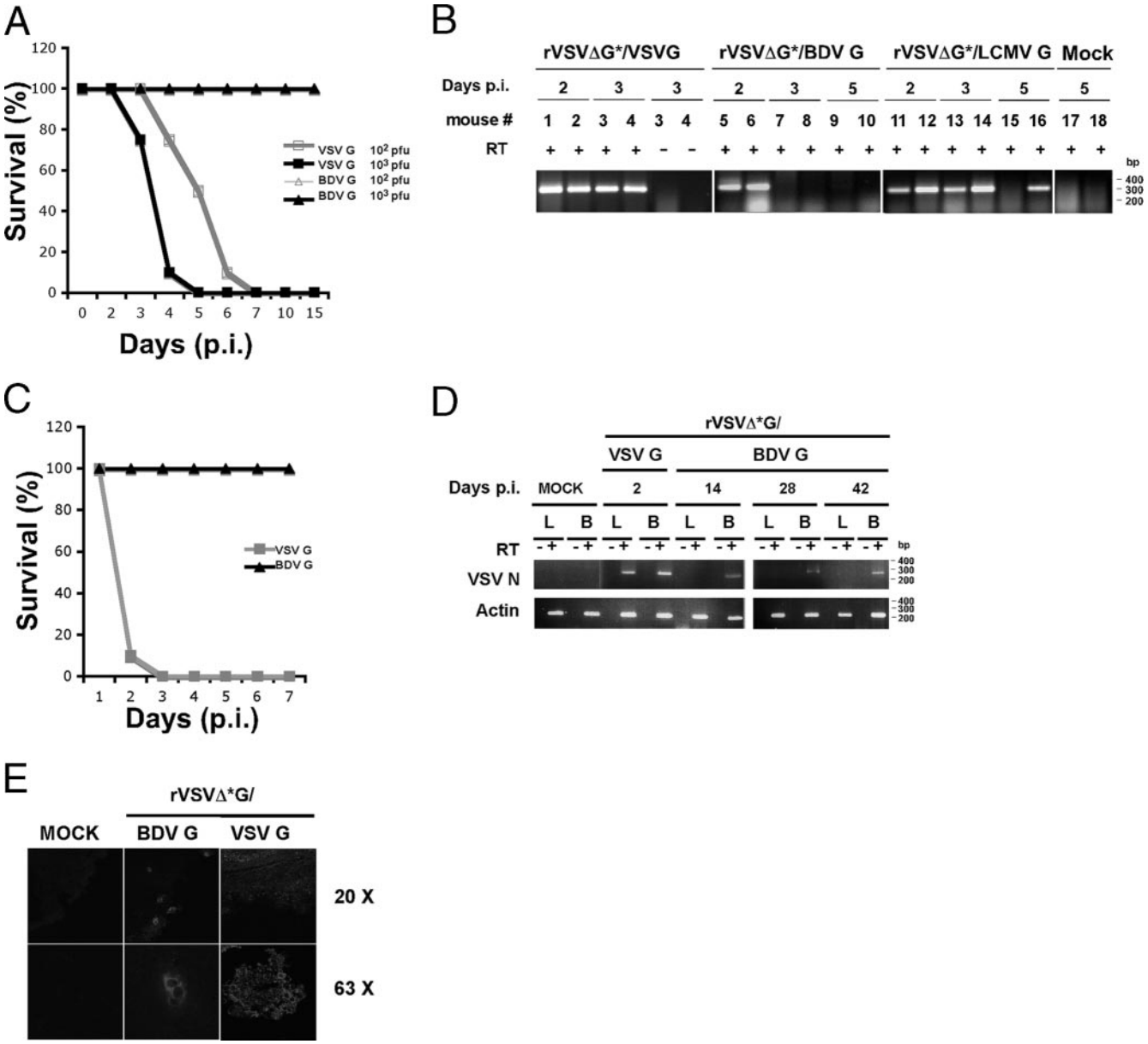

FIG. 6. Replication and virulence of rVSVΔG*/BDVG in mice. (A) Survival of B6 mice upon i.c. inoculation. Mice were inoculated with the indicated number of PFU of each virus and monitored daily. (B) Detection of viral RNA in brains of infected mice. B6 mice infected (i.c.) with the indicated rVSV were euthanized at the indicated days p.i. and RNA isolated from brain tissue. The presence of viral sequences was assessed by RT-PCR using specific primers to amplify a segment of the VSV N ORF. (C) Survival of IFNAR$^{-/-}$ mice upon i.c. inoculation of the indicated rVSVs. (D) Detection of viral RNA in brains and livers of infected IFNAR$^{-/-}$ mice. (E) Detection of viral antigen in brains of rVSV-infected IFNAR$^{-/-}$ mice. Brain sections from mice infected with either rVSVΔG*/BDVG or rVSVΔG*/VSVG at 2 weeks p.i. or 2 days p.i., respectively, were examined by IHC using an antibody to VSV N.

ficking to the cell surface (7, 41), which is the cellular site of VSV budding (2). Consistent with this notion, we observed that although expression levels of BDV G and VSV G were similar in cell lysates, the incorporation of BDV G into particles was severely restricted compared to that of VSV G (Fig. 4A). Nevertheless, the forms of BDV G protein incorporated into rVSVΔG*/BDVG virions resembled those observed in bona fide BDV particles (Fig. 4B).

Both rVSVΔG*/BDVG and BDV exhibited the same host cell range among the cell lines tested (Fig. 5A), suggesting that both viruses recognized the same cellular receptors. This view was further supported by results from neutralization assays (Fig. 5B) and competition experiments (Fig. 5C).

Results from infections of cultured cells indicated rVSVΔG*/BDVG was significantly attenuated compared to rVSVΔG*/VSVG (Fig. 2B and C) and also compared to rVSVΔG*/LCMVG (not shown). This attenuated phenotype was manifested by a delayed CPE as determined by both morphological changes in the cell monolayers (Fig.2Bi) and levels of apoptosis assessed by Annexin V expression levels (Fig.2Bii). In addition,

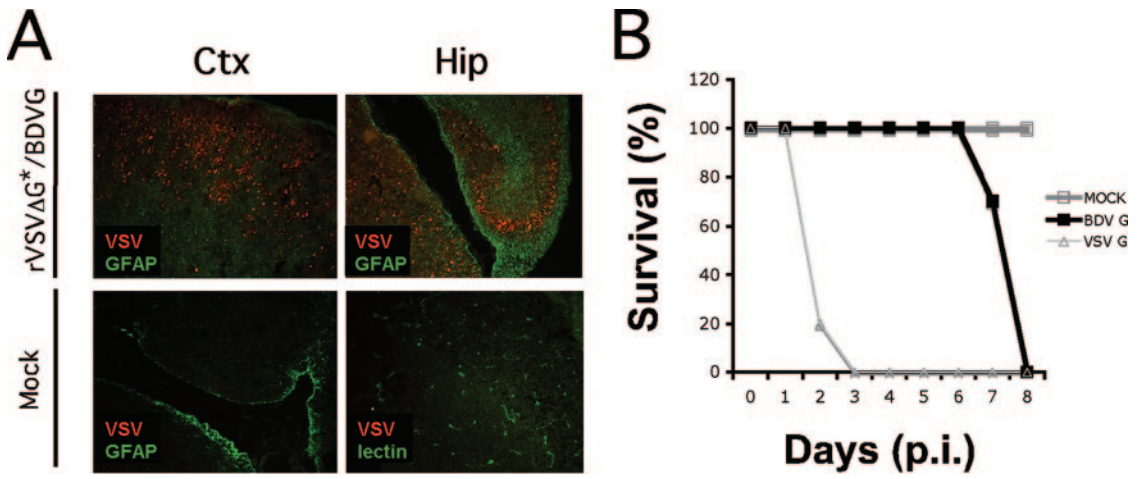

FIG. 7. Replication and virulence of rVSVΔG*/BDVG upon infection of newborn rats. (A) Detection of viral antigen in brains of rVSVΔG*/BDVG-infected newborn rats. Brain sections from rVSVΔG*/BDVG-infected or mock-infected control rats collected at day 5 p.i. were examined by IHC using an antibody to VSV N. Antibodies to GFAP and lectin were used to identify astrocyte and microglia cells, respectively, within the brain parenchyma. (B) Survival of newborn rats upon i.c. inoculation with rVSVΔG*/BDVG. Newborn rats were inoculated with rVSVΔG*/BDVG or rVSVΔG*/VSVG (1,000 PFU) and monitored daily. None of the mock-infected control rats ($n = 3$) exhibited morbidity throughout the duration of the experiment (not shown).

rVSVΔG*/BDVG plaques developed significantly slower and were smaller than those of rVSVΔG*/VSVG. The VSV M protein has been documented to play a central role in CPE, both cell rounding and apoptosis, associated with VSV infection (6, 11), although other viral components appear to contribute to VSV-induced CPE. Notably, the phenotypic features of rVSVΔG*/BDVG resembled those of some described VSV M mutants (3, 11). We therefore considered the possibility that during the rescue of rVSVΔG*/BDVG, unintended mutations were incorporated into its M ORF, which could result in a virus phenotype similar to that described for several VSV M mutants (3). However, sequence analysis revealed that rescued rVSVΔG*/VSVG and rVSVΔG*/BDVG had identical M ORFs (data not shown). Mutations within VSV M also have been shown to affect virus-host interaction in such a way that viral mRNAs accumulate at high levels but are translated less efficiently than those of wt VSV (3). Intriguingly, we observed a significantly increased N-mRNA/genome ratio in rVSVΔG*/BDVG-infected cells compared to that in cells infected with either rVSVΔG*/LCMVG or rVSVΔG*/VSVG (Fig. 3). However, VSVΔG*/BDVG-infected cells did not exhibit increased levels in viral polypeptide synthesis (Fig. 4A). This finding likely reflected the fact that reduced levels of genome RNA synthesis had a significant contribution to the altered N-mRNA/genome ratio. However, we cannot rule out that mRNAs produced by rVSVΔG*/BDVG also had lesser translation efficiencies than mRNAs produced by rVSVΔG*/VSVG.

The attenuated phenotype of rVSVΔG*/BDVG was dramatically manifested in infected mice. All the mice infected (i.c.) with 1,000 PFU survived, and none of them exhibited any noticeable morbidity (Fig. 6A). RT-PCR analysis readily detected viral RNA at day 2 p.i. in brains of rVSVΔG*/BDVG-infected mice (Fig. 6B), but rVSVΔG*/BDVG was cleared from the infected brains at day 3 p.i. One could speculate that propagation within the brain involves multiple rounds of infection, and a reduced propagation efficiency of rVSVΔG*/BDVG would give the host a window of opportunity to mount an efficient antiviral innate immune response that would clear rVSVΔG*/BDVG before the virus propagated extensively and induced sufficient cell damage to cause morbidity and mortality. Consistent with this hypothesis, we observed that rVSVΔG*/BDVG was able to persist for up to 42 days, the latest time examined, in the brains of IFNRA$^{-/-}$ mice (Fig. 6C to E). Notably, we could not detect viral RNA in blood or tissues, other than brain, in IFNRA$^{-/-}$ mice persistently infected with rVSVΔG*/BDVG (Fig. 6D). Whether replication of rVSVΔG*/BDVG outside the CNS is controlled by the appearance of neutralizing antibodies is currently under investigation. Moreover, histological analysis revealed that rVSVΔG*/BDVG replication within the CNS was highly restricted to certain neuronal populations by mechanisms that remain to be determined. Evidence indicates that the cytopathic nature of VSV, rather than immune-mediated pathology, appears to be the main factor contributing to VSV neuropathogenesis. Therefore, the restricted spread of rVSVΔG*/BDVG within the CNS of persistently infected IFNRA$^{-/-}$ mice may account for the lack of clinical symptoms in these mice. Consistent with this view, rVSVΔG*/BDVG, although attenuated with respect to rVSVΔG*/VSVG, caused 100% mortality by day 8 p.i. in newborn rats, which correlated with widespread virus propagation within the brain parenchyma.

The generation of rVSVΔG*/BDVG provides us with a unique tool for the identification of receptors that mediate BDV cell entry. In addition, the investigation of the mechanisms underlying the highly attenuated phenotype of rVSVΔG*/BDVG both in cultured cells and in mice may uncover novel aspects of BDV G-host cell interactions that could also have implications for the development of VSV-based vectors to deliver foreign genes and antigens.

ACKNOWLEDGMENTS

This is publication no. 18476 from the Molecular and Integrative Neuroscience Department (MIND) of The Scripps Research Institute.

We thank D. B. McGavern for his advice on the IHC procedures used for detection of viral antigen in brain tissue and B. Hahm for his help with the apoptosis studies.

M. Perez and R. Clemente contributed equally to this work.

This work was supported by NIH grants R21 AI064820 (J.C.D.L.T.) and R01 GM53726 (M.A.W).

REFERENCES

1. **Bajramovic, J. J., S. Munter, S. Syan, U. Nehrbass, M. Brahic, and D. Gonzalez-Dunia.** 2003. Borna disease virus glycoprotein is required for viral dissemination in neurons. J. Virol. **77:**12222–12231.
2. **Brown, E. L., and D. S. Lyles.** 2003. Organization of the vesicular stomatitis virus glycoprotein into membrane microdomains occurs independently of intracellular viral components. J. Virol. **77:**3985–3992.

2a. **Clemente, R., and J. C. de la Torre.** 2007. Cell-to-cell spread of Borna disease virus proceeds in the absence of the virus primary receptor and furin-mediated processing of the virus surface glycoprotein. J. Virol. **81:** 5968–5977.

3. **Connor, J. H., M. O. McKenzie, and D. S. Lyles.** 2006. Role of residues 121 to 124 of vesicular stomatitis virus matrix protein in virus assembly and virus-host interaction. J. Virol. **80:**3701–3711.
4. **Cubitt, B., and J. C. de la Torre.** 1994. Borna disease virus (BDV), a nonsegmented RNA virus, replicates in the nuclei of infected cells where infectious BDV ribonucleoproteins are present. J. Virol. **68:**1371–1381.
5. **de la Torre, J. C.** 2006. Reverse-genetic approaches to the study of Borna disease virus. Nat. Rev. Microbiol. **4:**777–783.
6. **Desforges, M., G. Despars, S. Berard, M. Gosselin, M. O. McKenzie, D. S. Lyles, P. J. Talbot, and L. Poliquin.** 2002. Matrix protein mutations contribute to inefficient induction of apoptosis leading to persistent infection of human neural cells by vesicular stomatitis virus. Virology **295:**63–73.
7. **Eickmann, M., S. Kiermayer, I. Kraus, M. Gossl, J. A. Richt, and W. Garten.** 2005. Maturation of Borna disease virus glycoprotein. FEBS Lett. **579:**4751–4756.
8. **Formella, S., C. Jehle, C. Sauder, P. Staeheli, and M. Schwemmle.** 2000. Sequence variability of Borna disease virus: resistance to superinfection may contribute to high genome stability in persistently infected cells. J. Virol. **74:**7878–7883.
9. **Fuerst, T. R., E. G. Niles, F. W. Studier, and B. Moss.** 1986. Eukaryotic transient-expression system based on recombinant vaccinia virus that synthesizes bacteriophage T7 RNA polymerase. Proc. Natl. Acad. Sci. USA **83:**8122–8126.
10. **Furrer, E., T. Bilzer, L. Stitz, and O. Planz.** 2001. High-dose Borna disease virus infection induces a nucleoprotein-specific cytotoxic T-lymphocyte response and prevention of immunopathology. J. Virol. **75:**11700–11708.
11. **Gaddy, D. F., and D. S. Lyles.** 2005. Vesicular stomatitis viruses expressing wild-type or mutant M proteins activate apoptosis through distinct pathways. J. Virol. **79:**4170–4179.
12. **Garbutt, M., R. Liebscher, V. Wahl-Jensen, S. Jones, P. Moller, R. Wagner, V. Volchkov, H. D. Klenk, H. Feldmann, and U. Stroher.** 2004. Properties of replication-competent vesicular stomatitis virus vectors expressing glycoproteins of filoviruses and arenaviruses. J. Virol. **78:**5458–5465.
13. **Gonzalez-Dunia, D., B. Cubitt, and J. C. de la Torre.** 1998. Mechanism of Borna disease virus entry into cells. J. Virol. **72:**783–788.
14. **Gonzalez-Dunia, D., B. Cubitt, F. A. Grasser, and J. C. de la Torre.** 1997. Characterization of Borna disease virus p56 protein, a surface glycoprotein involved in virus entry. J. Virol. **71:**3208–3218.
15. **Gosztonyi, G., and H. Ludwig.** 1995. Borna disease—neuropathology and pathogenesis. Curr. Top. Microbiol. Immunol. **190:**39–73.
16. **Hatalski, C. G., A. J. Lewis, and W. I. Lipkin.** 1997. Borna disease. Emerg. Infect. Dis. **3:**129–135.
17. **Kahn, J. S., M. J. Schnell, L. Buonocore, and J. K. Rose.** 1999. Recombinant vesicular stomatitis virus expressing respiratory syncytial virus (RSV) glycoproteins: RSV fusion protein can mediate infection and cell fusion. Virology **254:**81–91.
18. **Kiermayer, S., I. Kraus, J. A. Richt, W. Garten, and M. Eickmann.** 2002. Identification of the amino terminal subunit of the glycoprotein of Borna disease virus. FEBS Lett. **531:**255–258.
19. **Kobayashi, T., G. Zhang, B. J. Lee, S. Baba, M. Yamashita, W. Kamitani, H. Yanai, K. Tomonaga, and K. Ikuta.** 2003. Modulation of Borna disease virus phosphoprotein nuclear localization by the viral protein X encoded in the overlapping open reading frame. J. Virol. **77:**8099–8107.
20. **Kraus, I., M. Eickmann, S. Kiermayer, H. Scheffczik, M. Fluess, J. A. Richt, and W. Garten.** 2001. Open reading frame III of Borna disease virus encodes a nonglycosylated matrix protein. J. Virol. **75:**12098–12104.
21. **Kretzschmar, E., L. Buonocore, M. J. Schnell, and J. K. Rose.** 1997. High-efficiency incorporation of functional influenza virus glycoproteins into recombinant vesicular stomatitis viruses. J. Virol. **71:**5982–5989.
22. **Lawson, N. D., E. A. Stillman, M. A. Whitt, and J. K. Rose.** 1995. Recombinant vesicular stomatitis viruses from DNA. Proc. Natl. Acad. Sci. USA **92:**4477–4481.
23. **Perez, M., M. Watanabe, M. A. Whitt, and J. C. de la Torre.** 2001. N-terminal domain of Borna disease virus G (p56) protein is sufficient for virus receptor recognition and cell entry. J. Virol. **75:**7078–7085.
24. **Pinschewer, D. D., M. Perez, E. Jeetendra, T. Bachi, E. Horvath, H. Hengartner, M. A. Whitt, J. C. de la Torre, and R. M. Zinkernagel.** 2004. Kinetics of protective antibodies are determined by the viral surface antigen. J. Clin. Investig. **114:**988–993.
25. **Pletnikov, M. V., T. H. Moran, and K. M. Carbone.** 2002. Borna disease virus infection of the neonatal rat: developmental brain injury model of autism spectrum disorders. Front. Biosci. **7:**d593–d607.
26. **Pletnikov, M. V., S. A. Rubin, K. M. Carbone, T. H. Moran, and G. J. Schwartz.** 2001. Neonatal Borna disease virus infection (BDV)-induced damage to the cerebellum is associated with sensorimotor deficits in developing Lewis rats. Brain Res. Dev. Brain Res. **126:**1–12.
27. **Pletnikov, M. V., S. A. Rubin, M. W. Vogel, T. H. Moran, and K. M. Carbone.** 2002. Effects of genetic background on neonatal Borna disease virus infection-induced neurodevelopmental damage. I. Brain pathology and behavioral deficits. Brain Res. **944:**97–107.
28. **Richt, J. A., T. Furbringer, A. Koch, I. Pfeuffer, C. Herden, I. Bause-Niedrig, and W. Garten.** 1998. Processing of the Borna disease virus glycoprotein gp94 by the subtilisin-like endoprotease furin. J. Virol. **72:**4528–4533.
29. **Richt, J. A., I. Pfeuffer, M. Christ, K. Frese, K. Bechter, and S. Herzog.** 1997. Borna disease virus infection in animals and humans. Emerg. Infect. Dis. **3:**343–352.
30. **Robison, C. S., and M. A. Whitt.** 2000. The membrane-proximal stem region of vesicular stomatitis virus G protein confers efficient virus assembly. J. Virol. **74:**2239–2246.
31. **Rott, R., and H. Becht.** 1995. Natural and experimental Borna disease in animals. Curr. Top. Microbiol. Immunol. **190:**17–30.
32. **Rubin, S. A., J. R. Bautista, T. H. Moran, G. J. Schwartz, and K. M. Carbone.** 1999. Viral teratogenesis: brain developmental damage associated with maturation state at time of infection. Brain Res. Dev. Brain Res. **112:**237–244.
33. **Sambrook, J., E. F. Fritsch, and T. Maniatis.** 1989. Molecular cloning: a laboratory manual, 2nd ed. Cold Spring Harbor Laboratory Press, Cold Spring Harbor, NY.
34. **Schneemann, A., P. A. Schneider, R. A. Lamb, and W. I. Lipkin.** 1995. The remarkable coding strategy of borna disease virus: a new member of the nonsegmented negative strand RNA viruses. Virology **210:**1–8.
35. **Schneider, P. A., T. Briese, W. Zimmermann, H. Ludwig, and W. I. Lipkin.** 1994. Sequence conservation in field and experimental isolates of Borna disease virus. J. Virol. **68:**63–68.
36. **Schneider, U., M. Schwemmle, and P. Staeheli.** 2005. Genome trimming: a unique strategy for replication control employed by Borna disease virus. Proc. Natl. Acad. Sci. USA **102:**3441–3446.
37. **Schnell, M. J., L. Buonocore, E. Kretzschmar, E. Johnson, and J. K. Rose.** 1996. Foreign glycoproteins expressed from recombinant vesicular stomatitis viruses are incorporated efficiently into virus particles. Proc. Natl. Acad. Sci. USA **93:**11359–11365.
38. **Takada, A., C. Robison, H. Goto, A. Sanchez, K. G. Murti, M. A. Whitt, and Y. Kawaoka.** 1997. A system for functional analysis of Ebola virus glycoprotein. Proc. Natl. Acad. Sci. USA **94:**14764–14769.
39. **Weber, E. L., and M. J. Buchmeier.** 1988. Fine mapping of a peptide sequence containing an antigenic site conserved among arenaviruses. Virology **164:**30–38.
40. **Wehner, T., A. Ruppert, C. Herden, K. Frese, H. Becht, and J. A. Richt.** 1997. Detection of a novel Borna disease virus-encoded 10 kDa protein in infected cells and tissues. J. Gen. Virol. **78:**2459–2466.
41. **Williams, B. L., and W. I. Lipkin.** 2006. Endoplasmic reticulum stress and neurodegeneration in rats neonatally infected with borna disease virus. J. Virol. **80:**8613–8626.